

## COMBUSTION STABILITY CONTROL OF A SINGLE-PISTON FREE PISTON ENGINE GENERATOR

by

**Jinlong WANG, Jin XIAO<sup>\*</sup>, Yingdong CHENG, and Zhen HUANG**

<sup>a</sup> Key Laboratory for Power Machinery and Engineering of Ministry of Education,  
Shanghai Jiao Tong University, Shanghai, China

Original scientific paper  
<https://doi.org/10.2298/TSCI220404125W>

*Free piston engine generator is an effective alternative to conventional range extender, which is able to facilitate the transportation sector decarbonization attributed to its high thermal efficiency and ultimate fuel flexibility. However, due to the lack of crankshaft mechanism, stable and robust operation of free piston engine generator is difficult to achieve since various disturbances may exist during its operation. In this paper, a combustion stability control based on active disturbance rejection control algorithm was proposed for a single piston free piston engine generator. To develop this control, a thermodynamic model of the free piston engine generator system was calibrated and validated through experimental data. Afterward, a 2<sup>nd</sup> order active disturbance rejection control based speed control was developed by leveraging the developed free piston engine generator model. The proposed active disturbance rejection control was employed into multiple abnormal combustion scenarios through a simulation, including various fuel heat released, ignition positions and burn durations, aimed to verify the control ability of rejecting disturbances and enhancing the robustness of the free piston engine generator operation.*

Key words: *free piston engine generator, thermodynamic model, active disturbance rejection control, calibration and validation, speed tracking control*

### Introduction

Free piston engine generator (FPEG) that works as a range extender for electric vehicles is regarded as one of the promising technologies. Compared with the conventional internal combustion engine, the FPEG has the advantages of the simplest structure, the ultimate freedom of piston motion, as well as higher thermal and mechanical efficiency [1]. In addition, various renewable fuels can be employed into the FPEG to further facilitate the decarbonization due to its capability of achieving variable compression ratios [1]. In FPEG, trajectory of piston is no longer constrained by the crankshaft mechanism, but determined by the gas dynamics in combustion cylinder and the loading dynamics in real time. With numerous uncertainties, significant cycle-to-cycle variations and considerable periodic disturbances may exist during the combustion process, which makes it a remarkable challenge to achieve continuous and stable operation of the FPEG [2, 3].

---

<sup>\*</sup> Corresponding author, e-mail: xiaojin@sjtu.edu.cn

Currently, several control strategies have been employed to FPEG. Mikalsen [4] in Newcastle University developed a single piston free-piston engine generator. A piston motion controller was constructed to improve its dynamic performance. The controller response was based on a prediction of engine top dead center error instead of the measured value from the previous cycle. Compared with standard PI feedback control, the proposed control approach had excellent performance [5].

Some researchers [6-8] presented two control strategies based on the position feedback control method. In order to generate electricity and stabilize combustion, the first control approach adjusted the generating load coefficient to ensure piston motion follows the reference profile based on position and velocity of the piston. The second method was resonant pendulum type control method based on speed control and was activated only around the center of the piston stroke. The experimental results showed that the proposed control method is effective to achieve stable and continuous operation of FPEG.

Jia *et al.* [9] proposed cascade control strategy for the piston stable operation level, and proportional, integral, and derivative (PID) controllers were employed in both of the outer and inner loop. The simulation results showed that the proposed cascade control implemented in the FPEG had a good tracking performance, and it was improved in terms of the control delay, peak error and settling time.

Li *et al.* [10, 11] developed an active piston motion, namely the *virtual crankshaft*, and implemented it into an opposite-piston opposite-cylinder free piston engine. The experiment result demonstrated the effectiveness of the controller. Based on this achievement, Zhang *et al.* [12] in University of Minnesota proposed a trajectory-based combustion control method that is able to optimize the combustion process of multiple renewable fuels. The simulation results showed that the trajectory-based combustion control realizes the co-optimization of fuels and engine operation.

Lu *et al.* [13] developed a prototype of an opposed-piston engine generator. To stabilize the operation of such a system, an opposed-piston synchronous motion control strategy on the basis of master-slave position following and a compression ratio control based on ANN were proposed. The simulation results showed that the system reached stable operation and the compression ratio was well controlled.

Dinh and Ocktaeck [14] presented a dual FPEG. Their research described a simulation investigation of a predictive-fuzzy logic control method conducted on the dual FPEG. According to the results, predictive-fuzzy logic control is more effective than PID in terms of settling time, TDC error, and cycle-to-cycle variation.

Bo *et al.* [15] derived the non-linear dynamic model simulating the piston motion in a dual-piston free piston linear engine based on energy and force balance. The researchers designed a magnetoelectric load controller with motion stroke feedback to maintain the piston position in a predefined compression ratio by regulating the magnetoelectric force. The simulation results had been shown to have good control performance for the free piston linear engine system.

While many control strategies have been proposed by Ahmed *et al.* [16], these controls either are still based on the classical PID controls and require large efforts on the calibration of the related control gains, or demand a remarkable commitment to conduct system identification or develop neural network based models. These control strategies may not be sufficient for the FPEG tracking control, since the controlled plant is highly non-linear and possesses various uncertainties and disturbances during the combustion operation. As a result, an appropriate controller must have significant robustness to achieve an acceptable level of

tracking performance against a diversity of uncertainties and disturbances. This study is then motivated to construct a new tracking controller for FPEG, which emphasizes the ability to deal with multiple disturbances in an intelligent manner. The active disturbance rejection control (ADRC) was leveraged herein due to its reputation on dealing with system uncertainties and its capability of generating both excellent static and dynamic performance [17].

### Prototype test bench

The prototype of FPEG are presented in fig. 1. The test rig mainly consists of a two-stroke engine, a linear electrical machine, an air spring, a scavenge system, and a fuel supply system. The two-stroke engine employs in-cylinder direct injection and spark plug ignition technology. The linear electrical machine is a tubular type of linear permanent magnet synchronous motor-generator integration machine. Air spring is employed as the rebound device. Scavenge system adopts an external air source to provide constant air pressure 1.4 bar. The control system utilizes National Instruments Compact RIO-9039, a modular high performance embedded controller. The fuel-air equivalence ratio is employed as 1 in the test. Fuel injection timing is set as the time when the piston reaches 19.5 mm from the TDC, while the exhaust port is just closed. The spark timing is first set as the time when the piston reaches 9.5 mm. The prototype parameters are listed in tab. 1 [18]

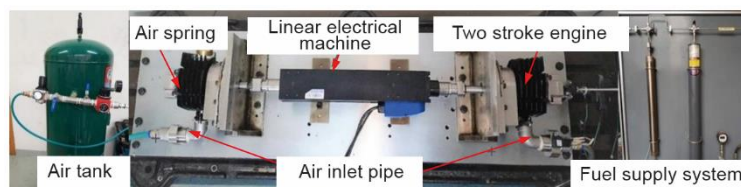


Figure 1. The FPEG prototype

Table 1. Prototype specification

Parameters	Value
Two-stroke engine bore [mm]	50
Air spring bore [mm]	50
Maximum stroke length [mm]	85
Maximum compression ratio	18.5
Linear machine force constant [N/A]	93
Back EMF constant [ $V\text{pkm}^{-1}\text{s}^{-1}$ ]	107.4
Linear machine resistance at 25 °C [ $\Omega$ ]	16.93
Air spring chamber intake pressure [bar]	1.5

### Calibration and validation of the model

The typical simulation model had been reported in [19-24], and the accuracy of FPEG model mainly depended on the thermodynamics model. Therefore, the focus of this section is to calibrate and validate the in-cylinder combustion process.

### Calibration of combustion process

For the sake of convenience, the gas pressure of the combustion chamber was set as the fixed scavenging pressure when the scavenging port is open. After the exhaust port closed, the variation of air pressure in the combustion chamber is given by [25]:

$$\frac{dP_{\text{eng}}}{dt} = -\gamma \frac{P_{\text{eng}}}{V_{\text{eng}}} \frac{dV_{\text{eng}}}{dt} + \frac{\gamma - 1}{V_{\text{eng}}} \left( \frac{dQ_{\text{in}}}{dt} - \frac{dQ_{\text{ht}}}{dt} \right) \quad (1)$$

where  $P_{\text{eng}}$  is the instantaneous air pressure in the combustion chamber,  $\gamma$  – the specific heat ratio,  $V_{\text{eng}}$  – the instantaneous volume of the combustion chamber,  $Q_{\text{in}}$  – the heat input from combustion, and  $Q_{\text{ht}}$  – the heat transfer to the engine wall.

The mass fraction burned  $\chi$  is usually represented by the exponential Wiebe function [19]:

$$\chi = 1 - \exp \left[ -a \left( \frac{t - t_0}{\Delta t} \right)^{m+1} \right] \quad (2)$$

The heat release rate can be written [19]:

$$\frac{dQ_{\text{in}}}{dt} = a \frac{m+1}{\Delta t} \left( \frac{t - t_0}{\Delta t} \right)^m \exp \left[ -a \left( \frac{t - t_0}{\Delta t} \right)^{m+1} \right] Q_{\text{in}} \quad (3)$$

where  $a$  and  $m$  are adjustable parameters,  $t_0$  – the initial time of combustion, and  $\Delta t$  – the combustion duration.

In Wiebe combustion function,  $a$  and  $m$  are adjustable parameters that determine the shape of the in-cylinder pressure curve. Constants of  $a$  and  $m$  have been employed by [19, 21, 22] to analyze the influence of load or combustion parameters on FPEG. The reported values of  $a$  and  $m$  are grouped into three cases in tab. 2.

**Table 2. values of a and m pairs in literature search**

Case	Values of $a$ and $m$	Reference
Case 1	$a = 5, m = 2$	[19, 21, 22]
Case 2	$a = 6.908, m$ was not mentioned	[26-28]
Case 3	$a$ and $m$ were not mentioned	[20, 23, 24]

The piston displacement profile obtained from the experimental test is imported into MATLAB/SIMULINK model. Change the mixture mass (absolute mass of air and fuel) to keep the maximum in-cylinder pressure constant. Then, the parameters  $a$  and  $m$  are adjusted to ensure that the shape of the simulated in-cylinder pressure agrees well with the experimental pressure measurement. Figures 2(a) and 2(b) shows the pressure shape with varying parameters  $a$  and  $m$ . When the parameter  $m$  decreases while  $a$  being a constant, the pressure profile tends to shift left. With  $m$  fixed and  $a$  decreasing, the pressure curve tends to shift right, especially after the maximum pressure point. Figure 2(c) illustrates the error of simulation and experi-

mental test in consecutive five cycles. The simulation curve is closest to the experiment profile when  $a = 6.908$  and  $m = 2$ , and this agreement can also be observed in fig. 2(d).

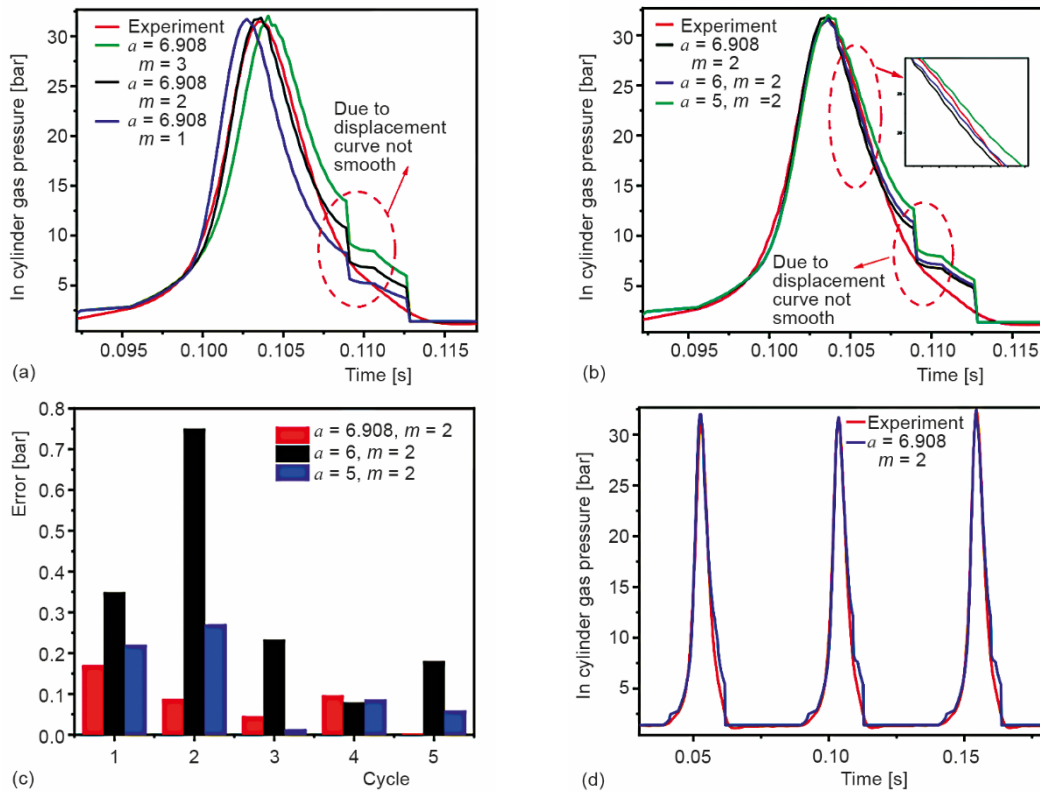


Figure 2. Combustion pressure calibration results

### Validation of modeling

The piston displacement, pressures in combustion chamber and air-spring chamber obtained from simulation model and test data are compared in fig. 3. The displacement from numerical model shows similar trends with test data, while the observed TDC are almost identical and the error of the bottom dead center can be controlled less than 0.55 mm. The simulated pressures in combustion chamber and air spring chamber agree well with the test data. The simulation model is highly accurate to predict the actual FPEG performance.

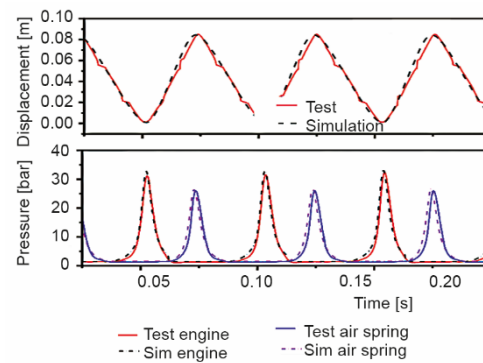


Figure 3. Comparison of experiment data and model results

## Active disturbance rejection control speed controller system

### Active disturbance rejection control introduction

The ADRC was proposed by Jingqing Han in 1998. Compared with classical PI controller design, the disturbances and non-linear dynamics are considered in ADRC. The ADRC has been utilized widely in many fields due to its high precision, fast response, simple structure, strong disturbance-rejection capability, and easy parameters adjusting. The ADRC is composed of three components as shown in fig. 4: tracking differentiator (TD), extended state observer (ESO), and non-linear states error feedback (NLSEF) [29, 30]. The 2<sup>nd</sup> order ADRC can be formulated [30]:

$$\begin{cases} \dot{x}_1 = x_2 \\ \dot{x}_2 = f + bu \\ y = x_1 \end{cases} \quad (4)$$

where  $f$  is the total disturbances of the plant (which compounds all the unknown disturbances and known dynamics),  $b$  – a constant, and  $u$  – the plant input. Figure 4 shows the ADRC structural schematic. In this figure,  $y_1, y_2$ , are tracking signals,  $z_1, z_2, z_3$  are the estimation of plan output  $y$ ,  $e_i$  ( $i = 1, 2$ ) is the tracking error,  $u_0$  is the output of NLSEF.

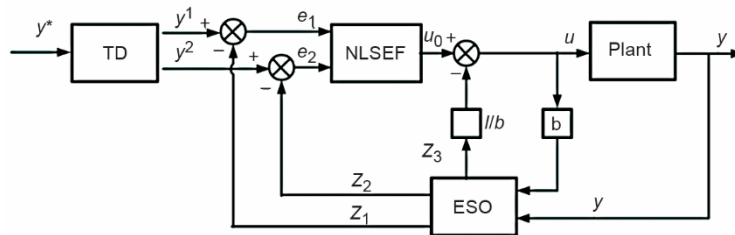


Figure 4. The ADRC structural schematic

### Active disturbance rejection control design for free piston engine generator

The linear machine is a critical component of the FPEG, which manipulates the electromagnetic force to achieve the continuous and stable operation of the system [7]. In this paper, the linear machine also works as the control plant and other forces acting on the piston are regarded as an external load.

Based on the linear machine model and Newton's second law, the following equation can be achieved:

$$\begin{cases} \frac{dv}{dt} = \frac{3}{2} \frac{\pi}{M\tau} [\Psi_m + (L_d - L_q)i_d]i_q - \frac{F_t}{M} \\ F_t = P_{eng}A_{eng} - F_f - P_{air\_spr}A_{air\_spr} \end{cases} \quad (5)$$

Since  $i_d^* = 0$  is usually employed in linear machine control, then  $i_d = 0$  is adopt here as well. Differentiate eq. (5) to get the following:

$$\frac{d^2v}{dt^2} = \frac{3}{2} \frac{\pi}{M\tau} \Psi_m \frac{di_q}{dt} - \frac{\dot{F}_t}{M} \quad (6)$$

The relative  $di_q/dt$  is shown [31]:

$$\frac{di_q}{dt} = \frac{1}{L_q}u_q - \frac{R}{L_q}i_q - \frac{\pi L_d}{\tau L_q}i_d v - \frac{\pi \Psi_m}{\tau L_q}v \quad (7)$$

So, eq. (8) can be obtained:

$$\frac{d^2v}{dt} = \frac{3\pi\Psi_m}{2M\tau L_q}u_q - \frac{3\pi\Psi_m R}{2M\tau L_q}i_q - \frac{3\pi^2\Psi_m^2}{2M\tau^2 L_q}v - \frac{\dot{F}_t}{M} \quad (8)$$

where  $R$  is the esistance of armature coil,  $u_q$  – the  $q$ -axis voltage, and  $F_t$  – the load force including friction force and gas forces in the combustion chamber and air spring chamber, respectively.

Let:

$$x_1 = v, \quad u = u_q, \quad f = -\frac{3\pi\Psi_m R}{2M\tau L_q}i_q - \frac{3\pi^2\Psi_m^2}{2M\tau^2 L_q}v - \frac{\dot{F}_t}{M}, \quad b = \frac{3\pi\Psi_m}{2M\tau L_q}$$

and substituting  $x_1$ ,  $u$ ,  $f$ , and  $b$  into eq. (4) yields:

$$\begin{aligned} \dot{x}_1 &= x_2 = \frac{dv}{dt} \\ \dot{x}_2 &= f + bu = -\frac{3\pi\Psi_m R}{2M\tau L_q}i_q - \frac{3\pi^2\Psi_m^2}{2M\tau^2 L_q}v - \frac{\dot{F}_t}{M} + \frac{3\pi\Psi_m}{2M\tau L_q}u_q \\ y &= x_1 = v \end{aligned} \quad (9)$$

For the 2<sup>nd</sup> order speed controller design for FPEG system, the variable to be controlled is the piston speed  $y = v$ , and the controller output, also known as the FPEG system input, is the  $q$ -axis voltage reference  $u = u_q$ . The speed loop is controlled by ADRC, and the current  $i_d$  is controlled by PI. Space vector pulse width modulation is employed to produce the switching signals of the inverter switches to generate a suitable voltage vector to achieve the above control objective  $u_q$ . Converting three-phase to two-phase frames can be done by Park and Concordia transformations, and vice versa.

## Results and discussion

To verify the disturbance rejection ability of ADRC, manipulated changes of the fuel heat released, the ignition positions and the burn durations in one cycle were simulated and the proposed ADRC was employed to study its effectiveness on multiple combustion variability. In these simulation results, the negative value of power means the generating state of the linear machine and conversely the positive value denotes the motor state for the linear machine. Normal combustion process is assumed for values of 100% fuel heat released, ignition position of 7.5 mm and burn duration of 8 ms.

### Fuel heat released

The effects of the fuel heat released on the speed trajectory tracking is shown in fig. 5. As can be seen in fig. 5, speed of piston has excellent consistency with reference in both the 50% fuel heat released and unfired cases. The alternate current was fluctuated in the

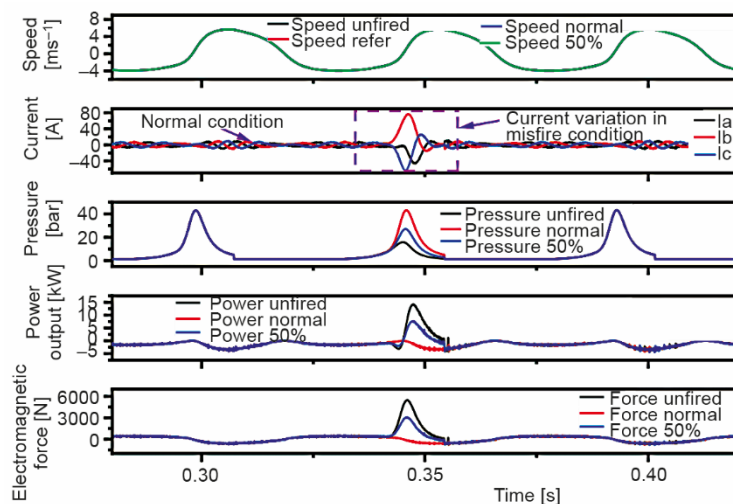


**Figure 5.** Effects of various fuel heat released on the speed trajectory tracking based on ADRC

abnormal scenarios to adapt the speed tracking. The maximum combustion pressure is directly proportional to the fuel heat released, since the input energy increased. Due to less cylinder gas pressure, the output power of linear machine in unfired and 50% fuel heat released are larger than normal combustion case before TDC. Then, in order to track reference velocity trajectory, the role of linear machine was changed from generator to electric motor in unfired and 50% fuel heat released cases. In these two cases, the maximum consumed electrical power is 7.67 kW and 14.16 kW, respectively. The electromagnetic force has a similar trend with output power. The maximum electromagnetic force is 3.06 kN in 50% fuel heat released and 5.41 kN in unfired case.

#### Ignition position

Figure 6 shows the effects of ignition position on the speed trajectory tracking based on ADRC. The ignition position is changed from 5 mm to 9.5 mm before the TDC. As is evident in fig. 6, there is no significant difference in speed tracking. The peak combustion pressure decreases when the corresponding ignition position is closer to the TDC. The output power of linear machine varies greater under these conditions. Compared with the standard normal combustion case, the working state of linear machine is summarized in tab. 3. Taking the TDC and in-cylinder pressure difference as the boundary, the linear machine switches between the generating state and the electric state in order to track velocity trajectory. For ex-

**Table 3.** The working state of linear machine

Item	bTDC		aTDC	
	Result	Linear machine	Result	Linear machine
$P-P_{\text{normal}}$	$\leq 0$	Generator	$\leq 0$	Motor
$P-P_{\text{normal}}$	$> 0$	Motor	$> 0$	Generator

ample, when the in-cylinder pressure,  $P$ , is less than the standard normal combustion pressure  $P_{\text{normal}}$  before TDC, the linear machine works as a generator. The greater the pressure variance, the larger the output or input power is required.

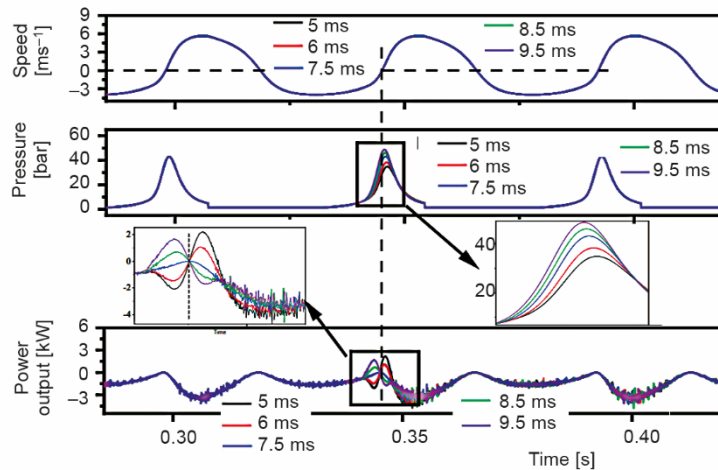


Figure 6. Effects of ignition position on the speed trajectory tracking base on ADRC

### Burn duration

The effects of different burn durations, ranging from 6 ms to 9 ms, on the speed trajectory tracking base on ADRC are shown in fig. 7. It can be observed that ADRC speed controller achieves a good speed tracking under burn duration disturbances. As the burn duration

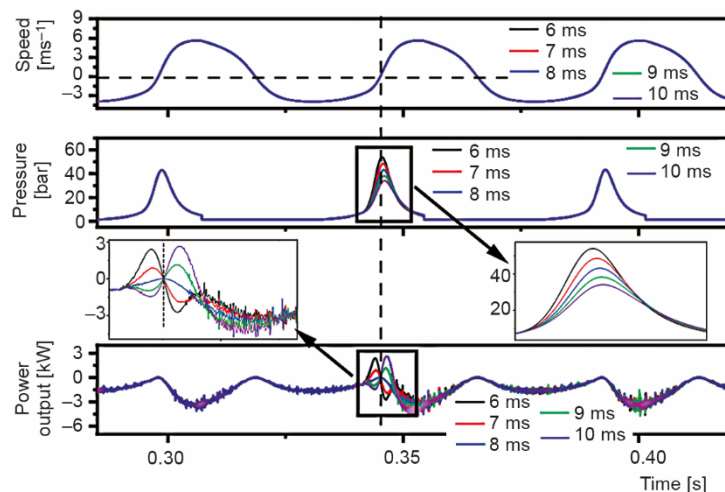


Figure 7. Effects of burn duration on the speed trajectory tracking base on ADRC

increases, the peak combustion pressure automatically decreases, or vice versa. The output power of linear machine has similar trends to the condition of ignition position variations. The criteria for linear machine changing the role between motor and generator can be referred to tab. 3. The adjustment process is automatically implemented and completed in one cycle, and its adjustment direction meets the need of the feedback control of speed.

### Discussion

To interpret the disturbance rejection ability of ADRC, it is necessary to research its strategy again. There is no doubt that the unknown disturbances have influence in the plant during system operation from eq. (10):

$$\frac{d^2v}{dt} = \frac{3\pi\Psi_m}{2M\tau L_q}u_q - \frac{3\pi\Psi_m R}{2M\tau L_q}i_q - \frac{3\pi^2\Psi_m^2}{2M\tau^2 L_q}v - \frac{\dot{F}_t}{M} = F[v, w(t)] + bu_q \quad (10)$$

where  $w(t)$  is an unknown disturbance.

In all existing conventions, it is required to obtain the analytical expression of  $F[v, w(t)]$  for feedback control design. However, the value of  $F[v, w(t)]$  can be estimated in real time in ADRC [30, 32].

Then, eq. (11) can be described [32]:

$$\frac{d^2v}{dt} = F[v, w(t)] + bu = F[v, w(t)] - bz_3(k) + bu_0 \quad (11)$$

Specially,  $z_3(k)$  is the estimate of  $F[v, w(t)]/b$  at time of  $t$ , then:

$$\frac{d^2v}{dt} \approx bu_0 \quad (12)$$

Such a strategy reduces the control of a complicated, perhaps non-linear, time-varying and uncertain process in eq. (10) to the simple problem in eq. (12) which can be easily controlled. In addition, when the disturbances that include the combustion process, air spring force, friction and unknown disturbances occur, linear machine is required to have enough energy to cover it even in misfire condition which consumes a lot of energy. Only then the ADRC will mitigate the influence of the disturbance and make sure the speed is tracking. In addition, it is equally important to adjust the control logic based on the ADRC control method to optimize energy distribution and parameters decoupling.

### Conclusions

In this study, based on the single piston free piston engine test rig, a thermodynamic model was calibrated and validated in MATLAB/SIMULINK. The validation procedure showed that the simulation results were in good correspondence with the test.

To verify the disturbance rejection ability of ADRC, the fuel heat released, ignition position and burn duration in one cycle were varied to study the influence on combustion variability, respectively. The simulation results showed that the linear machine changed the role between motor and generator to track the reference trajectory. Using the timely disturbance compensation of ADRC, it has been shown to be a promising candidate among competing solutions for FPEG control.

Currently, the control strategy was verified through a calibrated numerical model. In the future, it will be studied in the test bench to verify the disturbance rejection ability in practical world.

### Nomenclature

$A_{\text{air\_spr}}$	– sectional area of the air spring piston, [m <sup>2</sup> ]	$R$	– resistance of armature coil, [ $\Omega$ ]
$A_{\text{eng}}$	– sectional area of the engine piston, [m <sup>2</sup> ]	$t_0$	– time of starting combustion, [s]
$a$	– shape factor	$\Delta t$	– combustion duration, [s]
$f$	– total disturbances of the plant	$u_q$	– $q$ -axis voltage, [V]
$i_d$	– $d$ -axis current, [A]	$V$	– velocity of the piston, [m/s]
$i_q$	– $q$ -axis current, [A]		
$L_d$	– $d$ -axis inductance, [H]		
$L_q$	– $q$ -axis inductance, [H]		
$m$	– shape factor		
$M$	– mass of translator, [kg]		
$P$	– instantaneous pressure, [Pa]		
$P_{\text{air\_spr}}$	– gas pressure in the air spring chamber, [Pa]		
$P_{\text{eng}}$	– gas pressure in the combustion chamber, [Pa]		
$Q_{\text{in}}$	– heat input, [J]		
$Q_{\text{ht}}$	– heat transfer, [J]		

### Greek symbols

$\tau$	– pole pitch, [m]
$\Psi_m$	– magnet flux vector, [Wb]

### Acronyms

ADRC	– active disturbance rejection control
ESO	– extended state observer
FPEG	– free piston engine generator
NLSEF	– non-linear states error feedback

### Acknowledgements

This project is supported by the project of Science and Technology Commission of Shanghai Municipality (19511108500). We would like to thank the sponsors.

### Reference

- [1] Xiao, J., et al., Motion Characteristic of a Free Piston Linear Engine, *Applied Energy*, 87 (2010), 4, pp. 1288-1294
- [2] Kock, F., et al., The Free-Piston Linear Generator Potentials and Challenges, *MTZ Worldwide*, 74 (2013), 9, pp. 38-43
- [3] Guo, C., et al., Review of Recent Advances of Free-Piston Internal Combustion Engine Linear Generator, *Applied Energy*, 269 (2020), 6, 115084
- [4] Mikalsen, R., Roskilly, A., The Control of a Free-Piston Engine Generator, Part 1, Fundamental analyses, *Applied Energy*, 87 (2010), 4, pp. 1273-1280
- [5] Mikalsen, R., et al., Predictive Piston Motion Control in a free-Piston Internal Combustion Engine, *Applied Energy*, 87 (2010), 5, pp. 1722-1728
- [6] Kosaka, H., et al., Development of Free Piston Engine Linear Generator System Part 1 – Investigation of Fundamental Characteristics, SAE Technical Paper 2014-01-1203, 2014
- [7] Goto, S., et al., Development of Free Piston Engine Linear Generator System Part 2 – Investigation of Control System for Generator, SAE Technical Paper 2014-01-1193, 2014
- [8] Moriya, K., et al., Development of Free Piston Engine Linear Generator System Part 3 – Novel Control Method of Linear Generator for to improve Efficiency and Stability, SAE Technical Paper 2016-01-0685, 2016
- [9] Jia, B., et al., Piston Motion Control of a Free-Piston Engine Generator: A New Approach Using Cascade Control, *Applied Energy*, 179 (2016), 10, pp. 1166-1175
- [10] Li, K., et al., Active Motion Control of a Hydraulic Free Piston Engine, *IEEE/ASME Trans. Mech.*, 19 (2013), 8, pp. 1148-1159
- [11] Li, K., et al., Precise piston trajectory control for a free piston engine. *Control Engineering Practice*, 34 (2015), 1, pp. 30-38.
- [12] Zhang, C., et al., Trajectory-Based Combustion Control for Renewable Fuels in Free Piston Engines, *Applied Energy*, 187 (2017), 2, pp. 72-83
- [13] Lu, J., et al., Compression Ratio Control of an Opposed-Piston Free-Piston Engine Generator Based on Artificial Neural Networks, *IEEE Access*, 8 (2020), 6, pp. 107865-107875

- [14] Dinh, N. V., Ocktaeck, L., Piston Motion Control for a Dual Free Piston Linear Generator: Predictive-Fuzzy Logic Control Approach, *J. Mech. Sci. Technol.*, 34 (2020), 11, pp. 4785-4795
- [15] Bo, Y., et al., Control of Magnetoelectric Load to Maintain Stable Compression Ratio for Free Piston Linear Engine Systems, *Int. J. Struct. Stab. Dynam.*, 21 (2020), 2, 2150017
- [16] Ahmed, T. R., et al., A Review of Free Piston Engine Control Literature – Taxonomy and Techniques, *Alexandria Eng. J.*, 61 (2022), 10, pp. 7877-7916
- [17] Kai, S., Yanlei, Z., A New Robust Algorithm to Improve the Dynamic Performance on the Position Control of Magnet Synchronous Motor Drive, *Proceedings, 2<sup>nd</sup> International Conference on Future Computer and Communication (ICFCC)*, Wuhan, China, 2010, Vol. 3, pp. 268-272
- [18] Zhu, C. W., Research on Single-Piston Free Piston Linear Generator System, (in Chinese), M. Sc. thesis, Shanghai Jiao Tong University, Shanghai, China, 2019
- [19] Atkinson, C. M., et al., Numerical Simulation of a Two-Stroke Linear Engine-Alternator Combination, *SAE Transactions*, 108 (1999), 1, pp. 1416-1430
- [20] Fredriksson, J., Denbratt, I., Simulation of a Two-Stroke Free Piston Engine, SAE Technical Paper 2004-01-1871, 2004
- [21] Kim, J., et al., Simulation on the Effect of the Combustion Parameters on the Piston Dynamics and Engine Performance Using the Wiebe Function in a Free Piston Engine, *Applied Energy*, 107 (2013), 7, pp. 446-455
- [22] Jia, B., et al., Development and Validation of a Free-Piston Engine Generator Numerical Model, *Conversion and Management*, 91 (2015), 2, pp. 333-341
- [23] Mao, J., et al., Parameters Coupling Designation of Diesel Free-Piston Linear Alternator, *Applied Energy*, 88 (2011), 12, pp. 4577-4589
- [24] Hung, N. B., Lim, O. T., A Study of a Two-Stroke Free Piston Linear Engine Using Numerical Analysis, *Journal of Mechanical Science and Technology*, 28 (2014), 5, pp. 1545-1557
- [25] Feng, H., et al., Stable Operation and Electricity Generating Characteristics of a Single-Cylinder Free Piston Engine Linear Generator: Simulation and Experiments, *Energies*, 8 (2015), 1, pp. 765-785
- [26] Li, Q., et al., Simulation of a Two-Stroke Free-Piston Engine for Electrical Power Generation, *Energy & fuels*, 22 (2008), 5, pp. 3443-3449
- [27] Yuan, S., Wu, W., Simulation Study of a Two-Stroke Single Piston Hydraulic Free Piston Engine, *Proceedings, 7<sup>th</sup> International Conference on System Simulation and Scientific Computing*, Beijing, China, 2008, pp. 1244-1249
- [28] Huang, L., An Opposed-Piston Free-Piston Linear Generator Development for HEV, SAE Technical Paper 2012-01-1021, 2012
- [29] Su, Y., et al., Automatic Disturbances Rejection Controller for Precise Motion Control of Permanent-Magnet Synchronous Motors, *IEEE Transactions on Industrial Electronics*, 52 (2005), 6, pp. 814-823
- [30] Han, J., From PID to Active Disturbance Rejection Control, *IEEE Transactions on Industrial Electronics*, 56 (2009), 3, pp. 900-906
- [31] Boldea, I., *Linear Electric Machines, Drives, and MAGLEVs Handbook*, CRC press, Boca Raton, Fla., USA, 2013
- [32] Wu, D., et al., Tracking Control and Active Disturbance Rejection with Application to Noncircular Machining, *International Journal of Machine Tools and Manufacture*, 47 (2007), 12, pp. 2207-2217